PAPER Nr. : 67

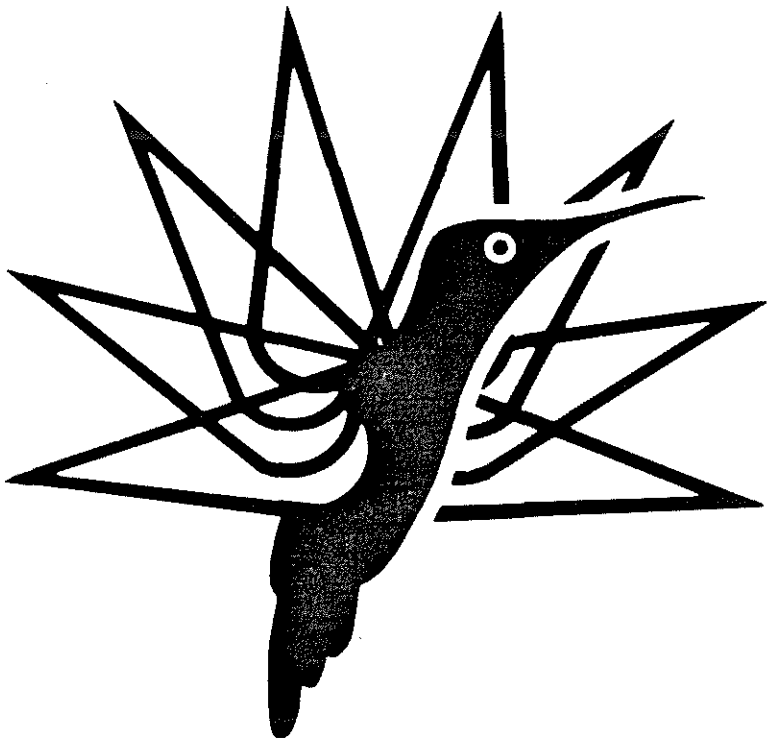

ON THE IDENTIFIABILITY OF HELICOPTER MODELS INCORPORATING HIGHER ORDER DYNAMICS

by

S.S. Houston

Flight Dynamics Division
Royal Aerospace Establishment
Bedford, MK41 6AE, UK

C.G. Black

Dept. of Aerospace Engineering
University of Glasgow
Glasgow, G12 8QQ, UK

FIFTEENTH EUROPEAN ROTORCRAFT FORUM

SEPTEMBER 12 - 15, 1989 AMSTERDAM

ON THE IDENTIFIABILITY OF HELICOPTER MODELS INCORPORATING HIGHER ORDER DYNAMICS

by

S S Houston
Flight Dynamics Division
Royal Aerospace Establishment
Bedford, MK41 6AE, UK

C G Black
Dept of Aerospace Engineering
University of Glasgow
Glasgow, G12 8QQ, UK

SUMMARY

Linearised mathematical models of the Puma helicopter operated by RAE Bedford have been identified from flight tests conducted in the hover. The test database includes collective pitch frequency sweep and step inputs. The aim has been to identify a 3 degree-of-freedom model of coupled body/coning/inflow response to collective. Two frequency-domain identification methods have been used with the data, and the paper explores how the identified stability and control derivatives vary with method, frequency range, parameter constraint, *a priori* estimates and test run. It is concluded that models of helicopter behaviour that include higher order dynamics can be identified successfully from flight, but care is required in the application of the methods and particularly in the interpretation of the results.

1. INTRODUCTION

Mathematical modelling of helicopters for handling qualities, performance and flight control has always been a challenging area, and is one which continues to demand increasing attention from the community. This is because deficiencies in fidelity are widespread, affecting the validity of piloted simulation and control law design, hence potentially increasing the cost of developing new aircraft. System identification is proving to be a powerful tool for assisting in the validation of rotorcraft mathematical models, including those which incorporate higher order dynamics associated with rotor flapping and air mass behaviour. Recent work at RAE Bedford and the University of Glasgow, has made significant contributions in this new area [1,2,3,4,5,6] and has highlighted potential difficulties associated with the identifiability of such models, which could conceivably limit the usefulness of system identification as a model validation tool. This Paper seeks to address these issues by example.

2. BACKGROUND

RAE Bedford and the University of Glasgow have been involved in the identification of helicopter mathematical models that incorporate higher order dynamics, for over two years. RAE have recently focussed on the vertical response to collective in the hover, [1,2,3,4], while Glasgow have examined forward flight cases in the mid-speed range [5,6]. Both organisations have had considerable success in identifying higher order effects, particularly inflow and flapping dynamics, to the extent that the results have been used to support the development of the RAE generic helicopter model HELISTAB/HELISIM [7]. The theme common to all of this work however has been a concern over model identifiability and robustness. Ref 8 reviews what is meant by the terms 'identifiability' and 'robustness' in the context of rotorcraft system identification, and what consequently may be required of an identification strategy. In general terms, identifiability may be thought of as indicating

whether or not a given model can be derived from the test data using a given identification method, and if it can, the term robustness can be applied to assess the degree to which the model parameters exhibit variation with method, data set frequency range, etc. These variations arise of course because of the uncertainty associated with experimental data and model structure, but are widened by the freedom to use engineering judgment at every stage in the identification process.

3. THEORETICAL MODELLING

The response of the helicopter to collective pitch inputs in hovering flight, can be described by a model incorporating those higher order dynamics of concern in this paper. The model incorporates first order inflow and vertical velocity response, together with second order coning. The model structure is written in constant coefficient, state-space form as

$$\dot{\underline{x}} = A\underline{x} + B\underline{u} \qquad (1)$$

where

$$A = \begin{bmatrix} i_{vi} & 0 & i_{\beta o} & i_w \\ 0 & 0 & 1 & 0 \\ f_{vi} & f_{\beta o} & f_{\beta o} & f_w \\ Z_{vi} & Z_{\beta o} & Z_{\beta o} & Z_w \end{bmatrix} \quad B = \begin{bmatrix} i_{\theta o} \\ 0 \\ f_{\theta o} \\ Z_{\theta o} \end{bmatrix} \qquad (2)$$

and

$$\underline{x} = [\ v_i \quad \beta o \quad \dot{\beta} o \quad w\ ]^T \ , \ \underline{u} = \theta o \qquad (3)$$

A is the system matrix, B the control matrix, $\underline{x}$ is the state vector, $\underline{u}$ the control vector, i_{vi}, f_{vi}, Z_{vi} are inflow, flapping and Z-force derivatives with respect to inflow, etc, θo is the collective pitch angle (rad), w is the vertical velocity (m/s positive down), v_i is the induced velocity (m/s positive down) and βo is the coning angle (rad). Chen and Hindson [9] provide analytical expressions for these stability and control derivatives, which exhibit the following relationships

$$Z_{vi} = -Z_w; \quad f_{vi} = -f_w; \quad i_w = -3/2\, R\, i_{\beta o}; \quad f_{\theta o} = -\Omega f_{\beta o}; \quad Z_{\theta o} = -\Omega\, Z_{\dot{\beta} o} \qquad (4)$$

R is the rotor radius (m) and Ω is the rotorspeed (rad/s). This model assumes constant rotorspeed, the derivatives do not take hinge offset into account, fuselage aerodynamics and

the interference between rotor and fuselage flowfields is neglected, the blades are assumed to be rigid and unsteady effects are not represented. This model formed the basis for the earlier RAE work in this area [1,2,3,4] which suggested that substantial improvements in the correlation between flight and theory could be obtained if some additional effects were included. These were:

a). empirical correction of the momentum-derived uniform component of inflow, to account for the real non-uniformity, tip loss and root cutout effects;
b). inclusion of lift deficiency factors to account for unsteady effects in the real wake;
c). reduction of blade first moment of mass, so that the rigid blade model made some approximation to the hub inertia force reactions experienced with real, flexible blades.

For this Paper the stability and control derivatives in the A and B matrices were obtained by a numerical forward and backward differencing of the full nonlinear equations (incorporating these additional features) which are as follows. The momentum expression for thrust, is

$$T = m_a \dot{vi} + 2\rho(3.142R^2)C'_t vi/k(vi/k - w + 2/3\,R\dot{\beta o}) \quad (5)$$

where T is rotor thrust (N), m_a is the additional air mass (kg), ρ is the air density (kg/m^3), C'_t is the thrust deficiency factor and k is the momentum empirical correction factor. From Johnson [10], C'_t is

$$C'_t = \frac{1}{1 + a\sigma/(16\bar{vi})} \quad (6)$$

where a is the blade lift-curve slope (1/rad), σ is the rotor solidity and $\bar{vi}$ is the induced velocity normalised by the rotor tip speed. The blade element expression for rotor thrust, to balance that given by equation (5) is

$$T = 1/4\,\Omega R\rho a\sigma(3.142R^2)(2/3\,\Omega R\theta o - vi + w - 2/3\,R\dot{\beta o}) \quad (7)$$

Again from Johnson [10], the equation for blade flapping is

$$\begin{aligned} I_\beta\ddot{\beta o} + \gamma\Omega I_\beta/8\,C'_1\dot{\beta o} - k_b M_\beta \dot{w} = {} & -I_\beta\gamma\Omega C'_1/(6R)\,vi - I_\beta\Omega^2\nu_\beta{}^2\beta o \\ & + I_\beta\gamma\Omega C'_1/(6R)\,w + I_\beta\Omega^2\gamma C'_\gamma/8\,\theta o \end{aligned} \quad (8)$$

where I_β is the blade flap inertia (kgm^2), γ is the Lock number, M_β is the blade first moment of mass (kgm), k_b is a factor on blade first flap moment and ν_β is the flap frequency ratio.

The hub force equation is

$$N I_\beta \Omega\gamma / (6mR)\, \dot{\beta}_o + N k_b M_\beta / m\, \beta_o - w = -N I_\beta \gamma \Omega / (4mR^2)\, v_i + N I_\beta \gamma \Omega / (4mR^2) w + N I_\beta \gamma \Omega^2 / (6mR)\, \theta_o - g \qquad (9)$$

where N is the number of blades, m is the mass of the helicopter (kg) and g is the acceleration due to gravity ($9.81 m/s^2$). C'_l is the lower harmonic loading limit of Loewy's lift deficiency function, given by

$$C'_l = \frac{1}{1 + 3.142\, \sigma / (4\, \bar{v}i)} \qquad (10)$$

With $k = k_b = C'_t = C'_l = \nu_\beta^2 = 1.0$, this model in linearised form is identical to that given in Ref 9. When configured as a Puma and trimmed in the hover and linearised with $k = 1.4$ and $k_b = 0.7$, (values suggested in Ref 4), the thrust and lift deficiency terms are $C'_t = 0.72$, $C'_l = 0.55$ and the A and B matrices corresponding to equation (2) are

$$A = \begin{bmatrix} -9.197 & 0 & -36.54 & 7.311 \\ 0 & 0 & 1 & 0 \\ -2.294 & -821.9 & -18.75 & 3.317 \\ 0.755 & -102.3 & 2.868 & -0.628 \end{bmatrix} \quad B = \begin{bmatrix} 589.0 \\ 0 \\ 517.5 \\ -79.14 \end{bmatrix} \qquad (11)$$

Note immediately, that two of the *relational* constraints shown in equation (4), specifically $f_{vi} = -f_w$ and $Z_{vi} = -Z_w$, are no longer valid. This is because C'_l is a function of vi. Equation (12) shows the equations of motion when Chen and Hindson's original model is configured as a Puma. Note that the modelling enhancements outlined above substantially modify the values of most of the derivatives. In particular, note that all bar one of the Z-force derivatives have opposite signs.

$$A = \begin{bmatrix} -11.44 & 0 & -39.27 & 7.856 \\ 0 & 0 & 1 & 0 \\ -5.692 & -848.6 & -32.16 & 5.692 \\ -0.168 & -177.8 & -1.618 & 0.168 \end{bmatrix} \quad B = \begin{bmatrix} 589.4 \\ 0 \\ 887.7 \\ 44.66 \end{bmatrix} \qquad (12)$$

4. THE FLIGHT TEST DATABASE AND IDENTIFICATION METHODS

The test database available contained pilot-generated frequency sweeps of the collective lever, conducted in a free-air hover. These were used for identification. Additionally, collective step inputs were used to provide a dissimilar input type for use in verifying the models identified from the sweeps. Seven separate frequency sweep runs were available for

analysis. The multiblade collective pitch and coning were derived from the individual measurements available from each blade. Except where indicated in the Paper, one of the seven sweep datasets available was used to illustrate the point under discussion. The dataset used is shown in Figure 1 which illustrates the pilot collective lever sweep, the multiblade coning and collective angles and the vertical acceleration.

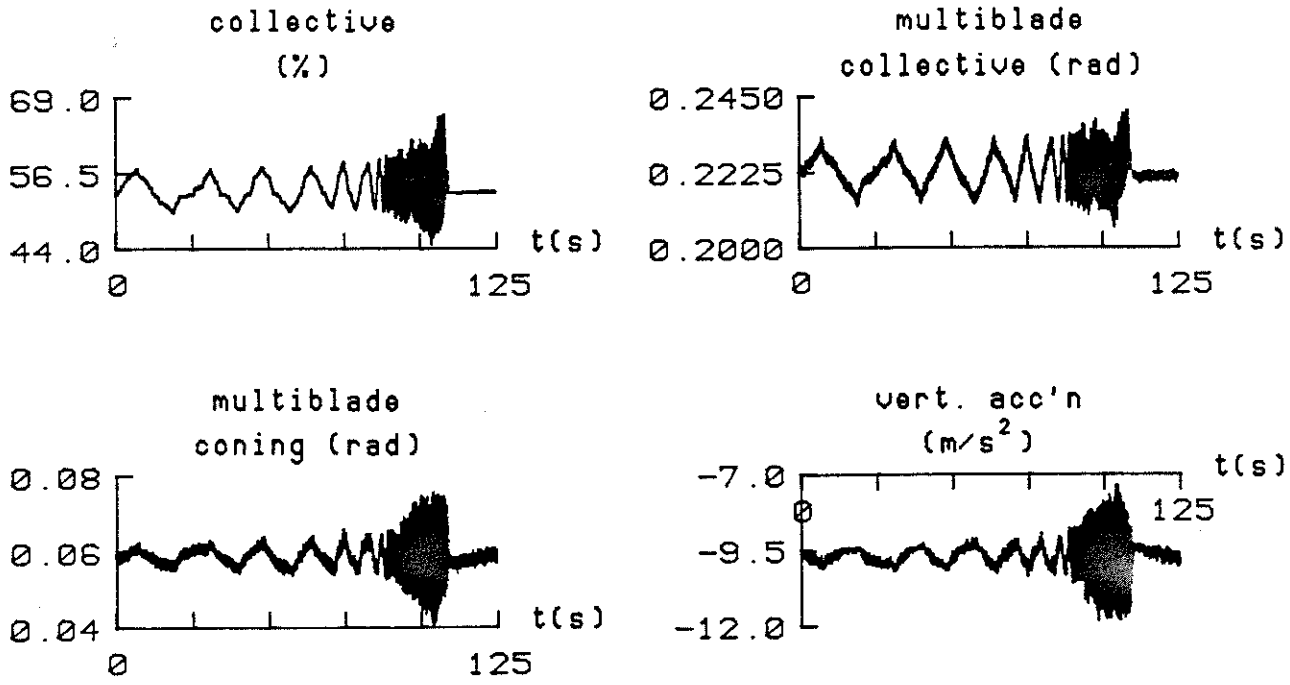

Figure 1 Collective lever frequency sweep and resulting aircraft response. Puma XW241, flight 757, run 10. Mass 5250kg, hover 3000ft.

The two identification methods used in this Paper were frequency-domain-based. The first method uses an output-error approach,where the outputs are based on the coning and vertical acceleration information. The state-space model is represented in terms of Fourier-transformed quantities, and an appropriate output-error identification carried out to determine the matrix coefficients. Details of this approach, in general, can be found in Ref 11, whilst mathematical details relating to this particular application can be found in Ref 12. The second method involved using time series analysis techniques to derive frequency responses representing transfer functions for the system, which were used with a model-matching process to find model parameters that allow the model structure to fit, in a least squares sense, the derived frequency responses. The latter approach which has been used at RAE is described in Ref [13]. Its application to this problem is detailed in Ref 2.

5. RESULTS

5.1 Comparison of transfer function matching and output-error method

With regard to the transfer function fitting approach, Figure 2 shows the flight-derived coning and vertical acceleration to collective frequency responses, together with the corresponding input-output coherences. Also shown is the best fit of this data in a least-squares sense, to the model structure given by equation (2). Any point with coherence less than 0.8 is not, however, used in the fitting process. All 14 derivatives were identified without constraint. Note that both coherence plots are very close to unity across most of the

frequency range, falling below 0.8 only at the first few frequency points, a region where the pilot's input has low content. Note also that the fit offered by the coupled 3 DOF model structure is excellent, again across the frequency range, with the exception of a few points at the very low frequency end of the response. Figure 3 shows corresponding results, to those illustrated in Figure 2, from the output-error approach, giving similarly good fits (phase comparisons have not been shown). It should be noted that some convergence difficulties were encountered with the output-error method, when attempts were made to estimate all fourteen parameters independently, and it was found to be necessary to fix the derivatives in the dynamic inflow equation. No measurements were available for the induced velocity vi, present as a state in the model. Alternative approaches include the use of a rank-deficient

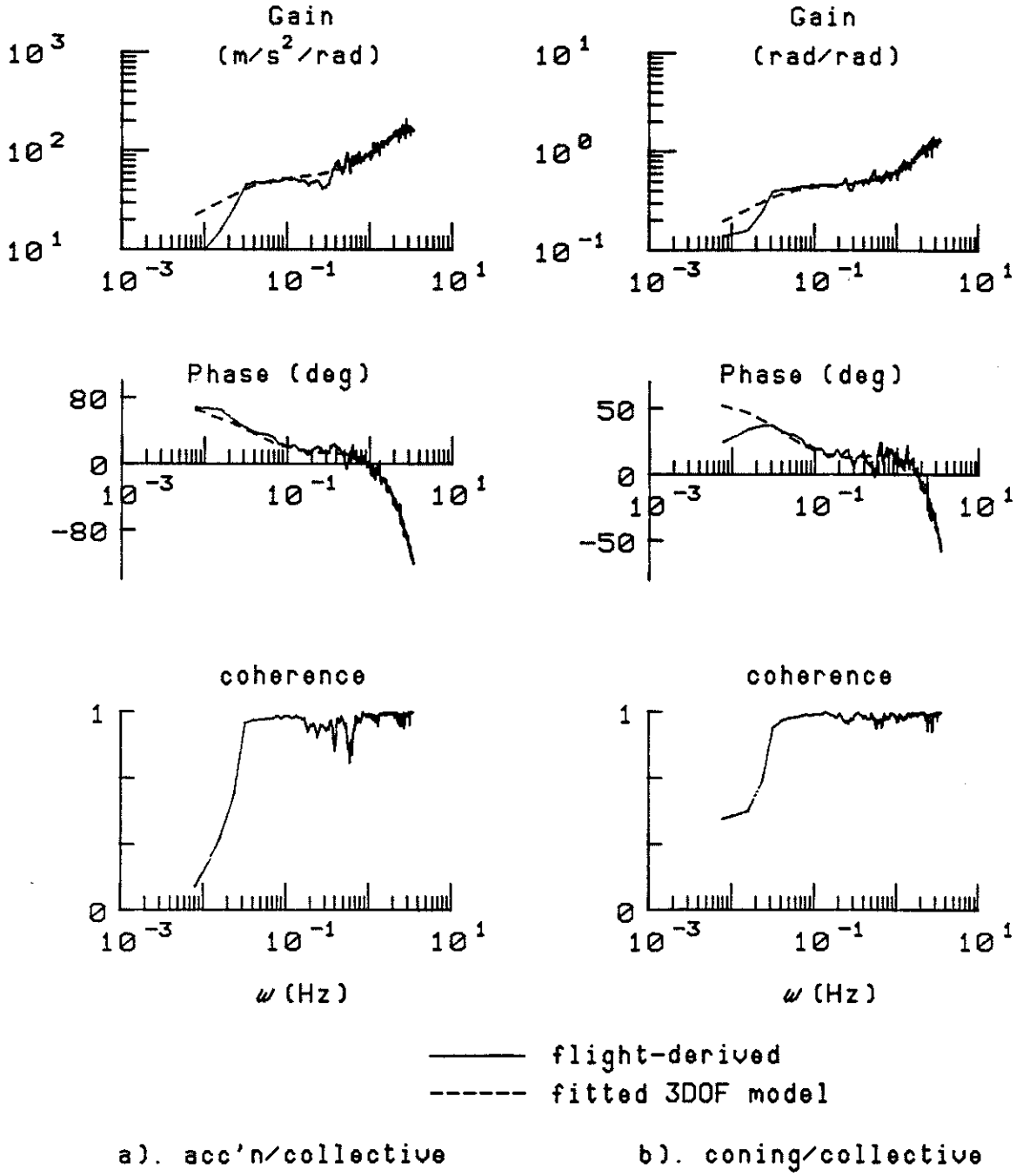

Figure 2 Frequency responses derived from collective sweep input, with best least-squares match given by 3 DOF model structure

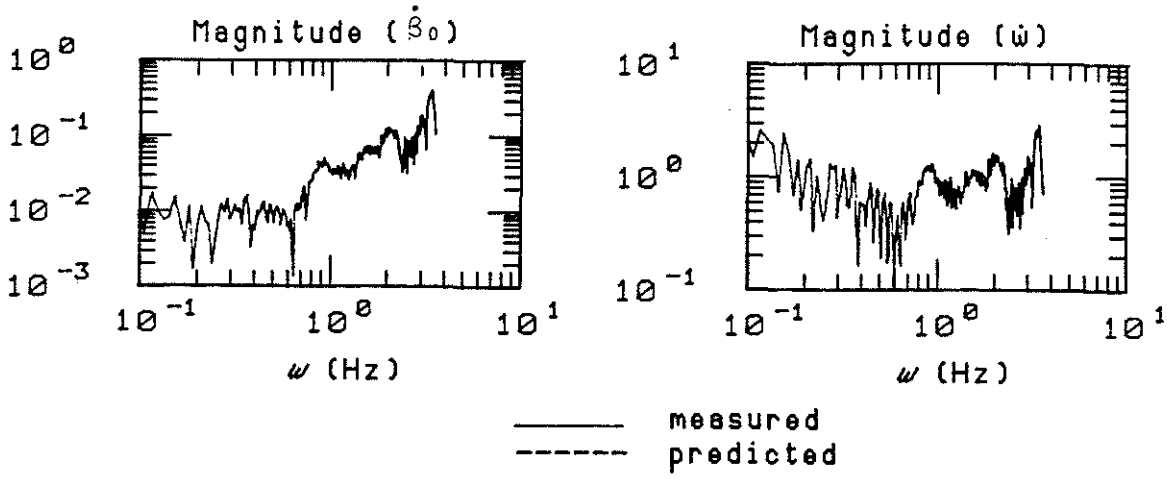

Figure 3 Comparison of measured and predicted magnitudes of the Fourier - transformed measurements

information matrix [14], or the incorporation of defined relationships into the model. Since the identified derivative values varied with the constraints used, the values identified by transfer function matching were used to fix the dynamic inflow equation derivatives in the output-error method, in order to lend consistency to the comparison between the two approaches.

TABLE 1 -- COMPARISON OF DERIVATIVES IDENTIFIED BY FREQUENCY RESPONSE AND OUTPUT-ERROR METHODS

Derivative	Theoretical Value	Frequency response[1]	Output-error[2]
i_{vi}	-9.197	-9.147 (0.0472)	-9.147[3] -
$i\dot{\beta}_o$	-36.54	-40.76 (0.5602)	-40.76[3] -
i_w	7.311	6.703 (0.0892)	6.703[3] -
$i_{\theta o}$	589.0	599.4 (3.0945)	599.4[3] -
f_{vi}	-2.294	-4.245 (0.0248)	-4.706 (0.28)
$f_{\beta o}$	-821.9	-836.7 (1.5973)	-857.1 (8.55)
$f_{\dot{\beta} o}$	-18.75	-24.47 (0.0855)	-25.15 (0.48)
f_w	3.317	4.635 (0.0443)	3.701 (0.88)
$f_{\theta o}$	517.5	682.8 (1.3974)	699.8 (12.7)
Z_{vi}	0.755	0.547 (0.0056)	0.291 (0.07)
$Z_{\beta o}$	-102.3	-96.46 (0.4640)	-101.1 (8.09)
$Z_{\dot{\beta} o}$	2.868	1.393 (0.0164)	4.833 (0.61)
Z_w	-0.628	-0.474 (0.0315)	-0.532 (0.11)
$Z_{\theta o}$	-79.14	-48.87 (0.3510)	-35.26 (6.95)

[1]parameter standard deviation in parentheses
[2]parameter standard deviation in parentheses
[3]values fixed at frequency-response method values

It can be seen that there is fairly good agreement between theory and experiment, and with only a few exceptions, that both identification methods give very similar derivative values. It would appear that the preferred approach to use is that of transfer function matching, since no constraints need to be applied for a viable solution to be obtained, unlike the output-error approach. However, with the use of appropriate constraints the output-error approach may be equally preferred. The question of the use of constraints, with output-error and transfer function approaches, is addressed in section 5.5 of the Paper.

5.2 Parameter sensitivity to test run

For illustrative purposes, the identification results presented so far, have focussed on only one of the seven sets of test data available. However, the other six sets do allow corresponding models to be identified, which in turn allows an assessment of the impact of any random run-to-run effects on the derivative values. This in turn gives an indication of how confident one might be in the results from any given single run. Should scatter be apparent, then the derivatives can be combined by an averaging process into a single model, to try and accomodate in a statistical way, the effects that have led to the variation in the derivative values. Run-to-run differences amongst the derivatives could be due to various things, but those of concern here are due to differences in rotor operating state and flight condition, or holes in the spectra of the particular sweep input that lead to frequency regions of poor coherence. In the approach used at RAE, the frequency response fitting process will discard such points, and it is this identification approach that was used to generate the results for this section.

The seven individual values for each derivative, available from each of the seven identified models, were treated as a sample set of data for which average, spread and sample standard deviation (SSD) were calculated. These results are shown in Table 2. Spread and SSD are expressed as a percentage of the average value. Perhaps the spread is hardly surprising, given that the sum of the squares of the mismatch between the fitted model's frequency response and that identified from flight, was for the poorest fit, almost three times that of the best fit. (No attempt has been made to explore correlation between the estimates, which could help to explain the spread).

In the case of each individual identified model, the variances associated with the derivative values were small, with the exception of that for i_{θ_0}. The frequency responses however, although each had the same form, had differences of detail. These were usually associated with regions of poor coherence which was itself a feature of the run-to-run comparisons. The spread in Table 2 above has to be viewed first of all in this context of differing run-to-run coherence, before any other contributions to the variability of the derivatives with run used, are considered. An additional point to note is that in general, the parameter standard deviations (being very small) do not reflect the actual spread among the seven identified models. This is consistent with other parameter estimation experience; the reader is referred to the work of Iliff and Main [15].

Analysis of the seven vertical acceleration to collective results in particular, revealed in four of the seven cases, that 15 to 25% of the points in the frequency response had coherence values less than 0.8 ie, played no part in the fitting process and the determination of the derivative values. By contrast, less than 5% of the points in the other three had coherence values less than 0.8. Accordingly, average, spread and SSD were recalculated using only these latter three cases. The results are shown in Table 3. Note that both the spread and SSD are considerably reduced in comparison with those given in Table 2. The spread of only one derivative out of the three models exceeds 30% of the average value, most being within 20%.

TABLE 2 SUMMARY OF DERIVATIVES IDENTIFIED FROM SEVEN TEST RUNS

Derivative	Theoretical value	Identified value[1]	Spread (%)	SSD (%)
i_{vi}	-9.197	-8.842(0.0571)	-21.6;+17.8	14.2
.				
$i_{\beta o}$	-36.54	-46.27(0.7113)	-11.9;+29.8	14.7
i_w	7.311	6.941(0.0900)	-7.1;+9.4	5.5
$i_{\theta o}$	589.0	593.07(3.7095)	-2.7;+2.8	2.1
f_{vi}	-2.294	-4.015(0.0247)	-31.0;+45.9	27.0
$f_{\beta o}$	-821.9	-819.77(2.7015)	-5.4;+7.2	4.5
.				
$f_{\beta o}$	-18.75	-23.48(0.1385)	-23.9;+30.2	17.7
f_w	3.317	4.301(0.0426)	-21.5;+34.7	19.7
$f_{\theta o}$	517.5	645.8(1.4591)	-15.1;+17.7	11.6
Z_{vi}	0.755	0.409 (0.0055)	-110.9;+56.1	53.6
$Z_{\beta o}$	-102.3	-110.2(0.5260)	-38.1;+69.9	33.8
.				
$Z_{\beta o}$	2.868	2.339(0.0300)	-62.0;+83.6	59.5
Z_w	-0.628	-0.402(0.0099)	-95.5;+43.9	45.2
$Z_{\theta o}$	-79.14	-39.61(0.3980)	-158.6;+76.0	73.7

[1]Averaged parameter standard deviation in parenthesis

TABLE 3 SUMMARY OF DERIVATIVES IDENTIFIED FROM 3 BEST DATA SETS

Derivative	Theoretical Value	Identified value	Spread (%)	SSD (%)
i_{vi}	-9.197	-8.797(0.0387)	-2.1;+4.0	3.4
.				
$i_{\beta o}$	-36.54	-45.63(0.5702)	-10.7;+5.7	9.2
i_w	7.311	6.595(0.0812)	-2.2;+0.6	2.0
$i_{\theta o}$	589.0	593.90(2.7173)	-0.7;+0.9	0.8
f_{vi}	-2.294	-3.963(0.0200)	-6.8;+7.1	6.2
$f_{\beta o}$	-821.9	-813.06(1.4626)	-1.8;+2.9	2.6
.				
$f_{\beta o}$	-18.75	-23.42(0.0725)	-2.3;+4.5	3.9
f_w	3.317	4.307(0.0380)	-9.1;+7.6	8.4
$f_{\theta o}$	517.5	648.2(1.2174)	-2.8;+5.3	4.6
Z_{vi}	0.755	0.553(0.0018)	-14.5;+15.6	15.0
$Z_{\beta o}$	-102.3	-86.47(0.4097)	-21.1;+11.6	18.3
.				
$Z_{\beta o}$	2.868	1.780(0.0168)	-21.7;+40 .9	35.4
Z_w	-0.628	- 0.402(0.0084)	-7.9;+6.4	11.0
$Z_{\theta o}$	-79.14	-54.60(0.0943)	-17.2;+27.7	24.2

Likewise only one SSD value exceeds 30% of the average, most being within 15%. Note however that the average values in Tables 2 & 3 are generally similar. A tentative conclusion from this analysis is that robust model parameters can be derived from data with less than 5% of the coherence values below 0.8. Conversely, if greater than 15% of the coherence points lie below 0.8, then the estimates are likely to exhibit wide spread in values. The results in Table 3 show that there is a slightly better correlation between theory and flight, than is displayed in Table 2, but for model validation, the true benefit of the results in Table 3 is that the spread in the identified values is much less. This gives a more robust set of derivative values which gives increased confidence in the use of the average values for the comparison with theory.

5.3 Parameter sensitivity to *a priori* estimates

In this section, a specific case is used to illustrate how different *a priori* estimates (that is, the starting guess used for the iterative parameter searches) of some derivatives can influence the identified values, and the resulting validation of the theoretical model. The transfer function matching approach is used, and the particular case involves the terms in the dynamic inflow equation

$$\dot{v}i = i_{vi}\, vi + i_{\beta o}\, \dot{\beta}o + i_{w}\, \dot{w} + i_{\theta o}\, \dot{\theta}o \qquad (13)$$

which will take substantially different values depending on the value of the additional air mass m_a that is used. Throughout this paper the value of air mass, m_a, used is that due to Carpenter and Fridovitch [16] - equation (14) shows the values of the dynamic inflow equation derivatives thus derived. The work of Pitt and Peters [17] gives a lower air mass value and the corresponding values are shown in equation (15).

$$\dot{v}i = -9.197\, vi - 36.54\, \dot{\beta}_0 + 7.311 w + 589.0\, \dot{\theta}_0 \qquad (14)$$

$$\dot{v}i = -14.347\, vi - 57.002\, \dot{\beta}_0 + 11.405\, w + 918.840\, \dot{\theta}_0 \qquad (15)$$

ie relative to equation (14), the derivatives are all increased by a factor of about 1.56. The derivatives identified using each set of *a priori* estimates are

$$\dot{v}i = -8.797\, vi - 45.631\, \dot{\beta}o + 6.595\, w + 593.896\, \dot{\theta}_0 \qquad (16)$$

$$\dot{v}i = -9.229\, vi - 51.653\, \dot{\beta}o + 9.643\, w + 911.012\, \dot{\theta}_0 \qquad (17)$$

where the former is that obtained with *a priori* values shown in equation (14), the latter using the values in equation (15). The results shown are based on the average of the three best datasets as defined in the previous section. The quality of fit of the transfer functions is the same in each case. This is an important result, and significant from the point of view of model validation. This is because with the exception of the derivative i_{vi}, the identified results are inconclusive regarding which value of m_a ought to be used in the theoretical model, the only compelling evidence to support the Carpenter and Fridovitch value, in both cases, being the term i_{vi}. This sensitivity to *a priori* estimates is undoubtedly due to the fact that the identification is performed without the aid of any inflow information. It is emphasised that these results are not the result of a convergence problem with the algorithm used to fit the 3 DOF model structure to the flight-identified frequency responses. The corresponding transfer function polynomials are identical in each case. The nature of this difficulty then is that the problem is underdetermined, having only two frequency responses (and hence transfer functions) with which to determine a state-space model that is actually fully described by three transfer functions.

This result implies that if the model is to be validated by comparison with identified derivatives, then the selection of the *a priori* estimates takes on some importance. The impact of this robustness issue on model validation can be assessed by examining the transfer function characteristics of the theoretical model, with both values of m_a. The value of m_a chosen for the theoretical model has a significant impact on the transfer function poles and zeros. Table 4 compares the poles of the theoretical model configured with both Carpenter and Fridovitch's as well as Pitt and Peters' value of m_a. In the case of the former, the inflow mode is considerably less well damped, although the coning mode is slightly better damped.

Table 5 compares the corresponding transfer function zeros. Perhaps the only important difference, (since they lie in the right-half, unstable part of the s-plane) is in the complex pair in the vertical velocity to collective transfer function.

TABLE 4 -- COMPARISON OF THEORETICAL MODEL TRANSFER FUNCTION POLES

Mode	Carpenter-Fridovitch	Pitt-Peters
inflow	-11.558	-18.417
coning	-8.411± 25.344i	-7.565±24.908i
heave	-0.196	-0.202

TABLE 5 COMPARISON OF THEORETICAL MODEL TRANSFER FUNCTION ZEROS

Transfer function	Carpenter-Fridovitch	Pitt-Peters
vi/θo	(0.752);(6.480±27.723i)	(0.752);(6.480±27.723i)
βo/θo	(0.094);(-6.800)	(0.095);(-10.506)
w/θo	(-4.991);(0.608±39.016i)	(-7.651);(0.876±39.385i)

5.4 Parameter sensitivity to frequency range

Figure 4 shows how all fourteen derivatives in the model vary with the frequency range used, when identifying models using the transfer function matching approach. In all cases, the lowest frequency point forms the start of the frequency range, and each derivative is plotted against the upper limit in the frequency range. For convenience, the derivatives have all been normalised by the corresponding theoretical value given in equation (11). Normalised values of 1 indicate that theory and flight correlate identically - any value less than zero would indicate that theory and flight derivatives had opposite sign. The agreement between theory and experiment is discussed later; in this section, the important feature examined is the point at which the derivative values cease to vary significantly with increasing frequency. With the coning and inflow derivatives, there is a definite trend with increasing frequency, and in these cases the identified derivatives cease to vary significantly with increasing frequency above about 3Hz. Such a trend is not as obvious in the Z-force derivatives, and it is here that evidence suggests that the derivatives are still changing and therefore that even 3.5Hz is an insufficient frequency range for robust identification of these derivatives. Perhaps such a result is not entirely surprising - it is the experience with these model-matching methods at RAE that resonant peaks, and just as importantly the following gain and phase 'roll-off', generally have to be included to define properly any model. In the particular case examined in this Paper, the resonant peak in coning and vertical acceleration to collective is around 3-3.4Hz, consistent with the result just observed. This tends to confirm then, that one ought to identify across a frequency range appropriate to the bandwidth of the model. This is 3-4Hz with this model because of the impact of the coning dynamics, which have a natural frequency just slightly in excess of 3Hz.

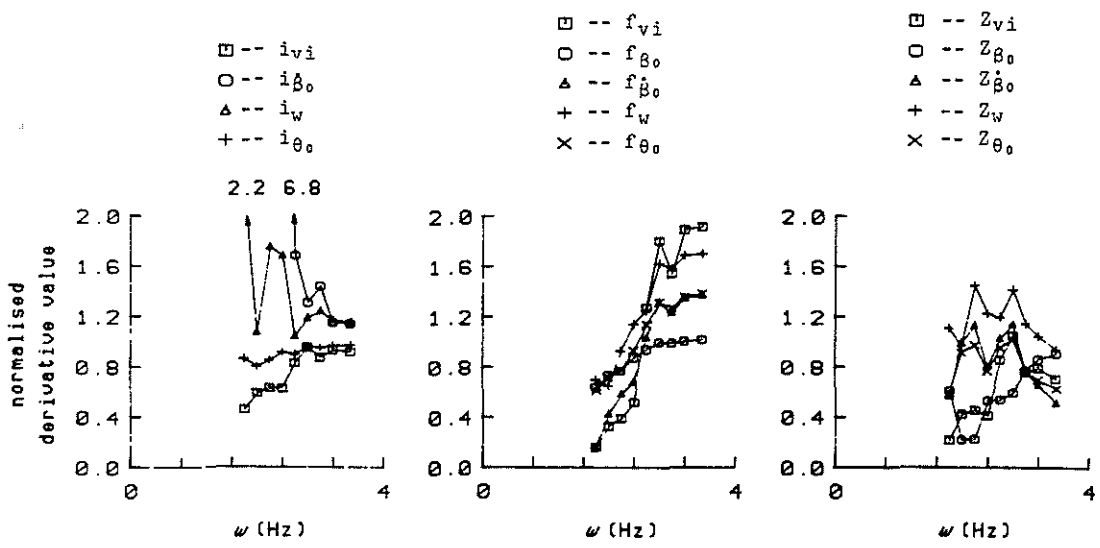

Figure 4 Sensitivity of parameter estimates to frequency range - transfer function matching method

5.5 Parameter sensitivity to constraints

Constraining parameters is a common feature of identification approaches. Sometimes it is done when limited information is available and the model has many parameters, and the method used may not converge onto a realistic solution, if at all. In such cases, a derivative may be fixed at a value that is theoretically based. Alternatively, the structure of the model to be validated may suggest some natural constraints that can be used to minimise the number of independent terms to be identified. Both types of constraint are explored in this section.

Firstly, with reference to equation (4), it can be seen that there are five *relational* constraints. Previous work [2] however, showed that the constraints involving the control terms were not appropriate to invoke, (this was attributed to unmodelled engine/rotor governing dynamics) leaving three. Solutions based on this approach were obtained using the transfer function matching method, and the result is shown in Table 6. Note that there are some differences, but in general both models are very similar. In the context of model validation, the differences shown in Table 6 are not significant.

Secondly, one of the derivatives was fixed at a theoretical value. *Numerical* constraint such as this are a common feature in identification, but is used here to illustrate that, across a broad frequency range, two very different solutions can have apparently very similar frequency responses. In addition, it is shown that choice of one of the models over the other has a significant impact on model validation. The results presented can be found in the earlier work [2,3,4] and are included in this Paper for completeness. The theoretical model derivatives are those given by Chen and Hindson's original model configured as a Puma ie

equation (12). Further, the identified models were derived using a different test run to that used elsewhere in this Paper. Finally, the three constraints $f_{vi} = -f_w$, $Z_{vi} = -Z_w$ and $i_{\beta o} = -3/2Ri_w$ were active in the identification. The results are given in Table 7. One of the models has been identified with $Z_{\theta o}$ constrained at the theoretical value. This is compared with the solution obtained with $Z_{\theta o}$ free where it took the opposite sign. It is clear that theory, as given by Chen and Hindson's equations, ie without any of the additional modelling features outlined in this Paper, displays much better correlation with the model identified with $Z_{\theta o}$ constrained, than it does with the other model. In fact, it could almost be argued from this result that the theoretical model does not need any improvement.

TABLE 6 -- COMPARISON OF SOLUTIONS - 3 RELATIONAL CONSTRAINTS VS. NO. CONSTRAINTS

Derivative	Theoretical Value	Unconstrained	3 constraints
i_{vi}	-9.197	-9.147 (0.0472)	-9.271 (0.0500)
$i_{\beta o}$	-36.54	-40.76 (0.5602)	-35.79 (0.2709)
i_w	7.311	6.703 (0.0892)	7.161 -
$i_{\theta o}$	589.0	599.4 (3.0945)	578.2 (2.8634)
f_{vi}	-2.294	-4.245 (0.0248)	-4.866 -
$f_{\beta o}$	-821.9	-836.7 (1.5973)	-837.2 (0.3895)
$f_{\beta o}$	-18.75	-24.47 (0.0855)	-25.46 (0.1196)
f_w	3.317	4.635 (0.0443)	4.866 (0.0200)
$f_{\theta o}$	517.5	682.8 (1.3974)	705.2 (1.5643)
Zvi	0.755	0.547 (0.0050)	-0.497 (0.0100)
$Z_{\beta o}$	-102.3	-96.46 (0.4640)	-102.5 (0.4709)
$Z_{\beta o}$	2.868	1.393 (0.0164)	1.131 (0.0100)
Z_w	0.755	0.547 (0.0315)	-0.497 (0.0100)
$Z_{\theta o}$	-79.14	-48.87 (0.3510)	-43.28 (0.4254)

(parameter standard deviation in parentheses)

This assessment is reinforced by Figure 5, which appears to show that the model identified with $Z_{\theta o}$ constrained gives, at least by visual inspection, just as good a fit with the flight-derived frequency response as the model identified with $Z_{\theta o}$ free, certainly up to 3Hz. In this figure, the vertical acceleration to collective gain of both identified models shown in Table 7, is compared with the frequency response derived from the sweep data. (Here the analysis is optimised to focus on frequencies higher than the 3.5Hz used in the identification). However, differences become visually apparent beyond 3Hz and it can then be argued that the characterisation of the Puma obtained with $Z_{\theta o}$ free is the more appropriate one for model validation. It is clear then, that the use of a constraint can substantially affect

the derivative values, and so care must be exercised if circumstances are such that this has to be done, eg if an acceptable solution cannot be obtained because of insufficient state information, such as the case in section 5.3 above. In this case, the impact on model validation conclusions are significant. Where a fixed constraint has to be used, a potential way forward would be to identify a family of models, effectively attempting to validate theory in a parametric manner.

TABLE 7 --USE OF NUMERICAL CONSTRAINTS - COMPARISON OF TWO IDENTIFIED MODELS WITH THEORY

Derivative	Theory	Identified value [1]	Identified value [2]
i_{vi}	-11.441	-9.809	-8.553
.			
$i_{\beta o}$	-39.272	-41.955	-35.340
i_w	7.856	8.393	7.070
$i_{\theta o}$	589.369	606.252	578.833
f_{vi}	-5.692	-5.650	-4.107
$f_{\beta o}$	-848.588	-886.946	-803.720
.			
$f_{\beta o}$	-32.162	-31.219	-22.517
f_w	5.692	5.650	4.100
$f_{\theta o}$	887.682	764.270	638.582
Z_{vi}	-0.168	-0.233	0.449
$Z_{\beta o}$	-177.799	-205.271	-109.410
.			
$Z_{\beta o}$	-1.618	-0.436	2.619
Z_w	0.168	0.233	-0.449
$Z_{\theta o}$	44.655	44.655	-44.390

[1] $Z_{\theta o}$ fixed at theoretical value

[2] $Z_{\theta o}$ free

It is interesting to note that time-domain comparison of both models' prediction of the helicopter's response to a step input, is unable to resolve this potential robustness problem. It might be thought that this would be a particularly efficatious way of deciding which of these two models is the more appropriate representation of the Puma, because of the difference in their respective $Z_{\theta o}$ derivatives. In response to a given step, one would give a positive increment in acceleration at time zero, as opposed to the other which would give a negative increment. Under ideal circumstances, this difference could be observed in the initial vertical response to the step input, and the more appropriate model would then be apparent. In this case however, two aspects of the problem mask this feature. Firstly, the differences between the two models manifest themselves only at very high frequency, which means that inputs

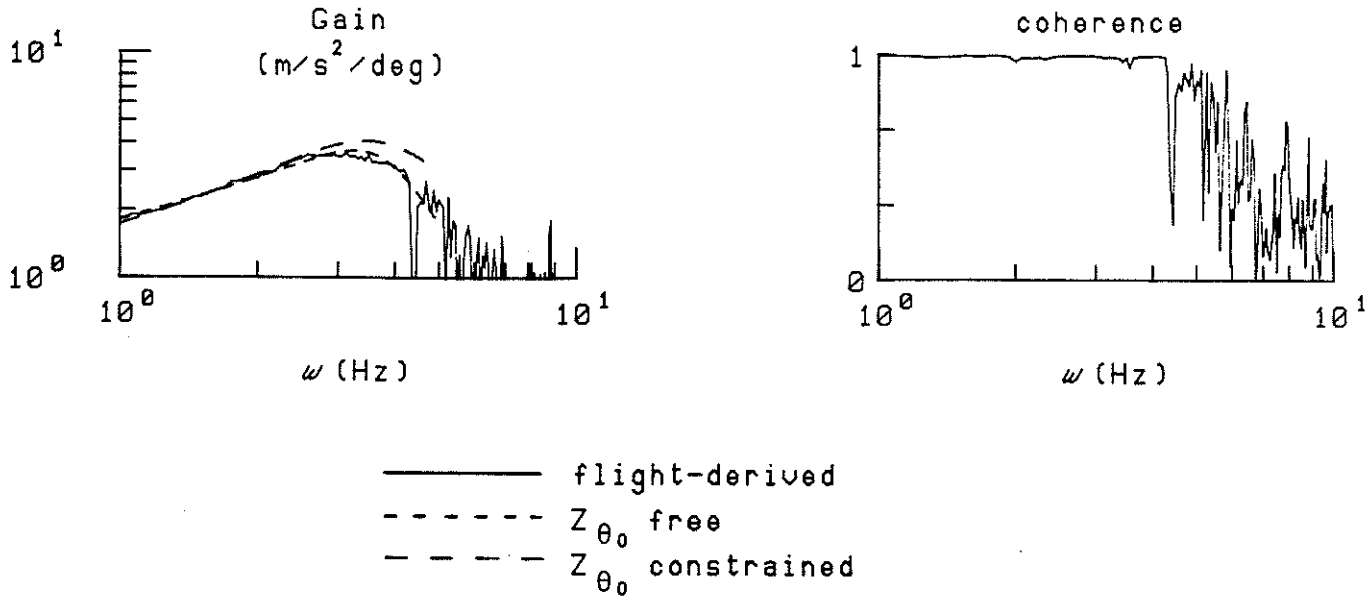

Figure 5 Vertical acceleration to multiblade collective frequency response - comparison of models identified with fixed and free $Z_{\theta o}$

other than pure steps are unlikely to have the frequency content required. Secondly, pilot neuromuscular and actuation system lags do tend to result in 'nominal' steps actually appearing as ramps. Results to illustrate this are shown in Figure 6, which compares the vertical acceleration response to a nominal step input in collective, measured in flight, with that predicted using both identified models. The input only has the frequency content to excite both models at the lower frequencies where both models give an excellent match with the flight-derived frequency response.

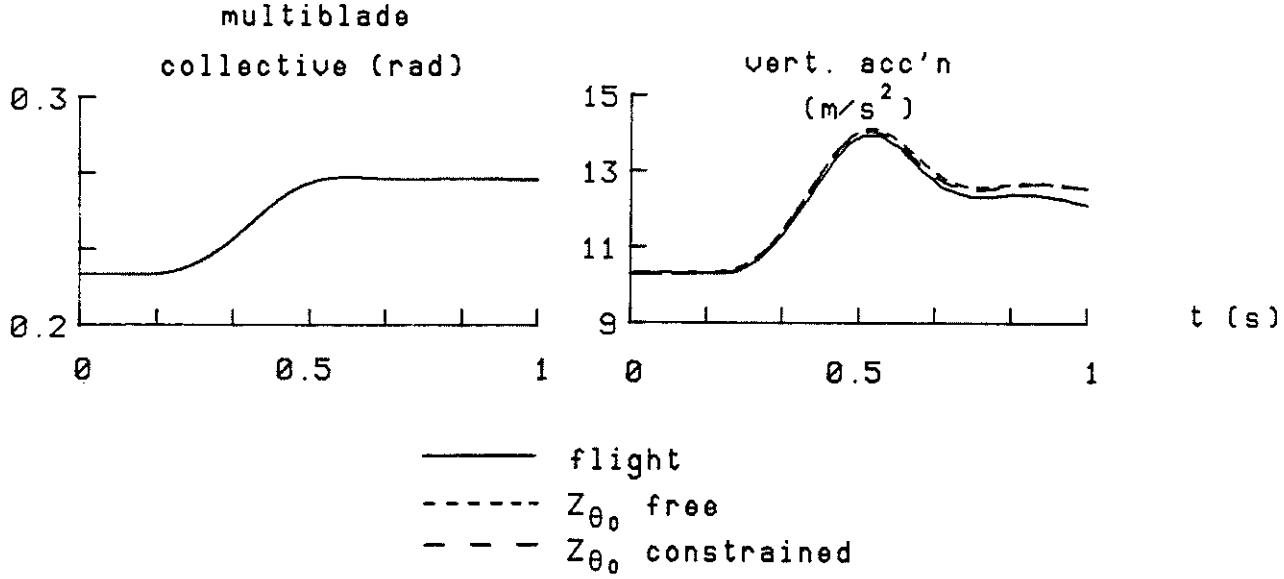

Figure 6 Comparison of the prediction of the response to a step input given by both identified models - transfer function matching method

The final example in this section concerns the output-error method. When a rank-deficient information matrix is used for the output-error method (indicating, on the basis of the data, implicit relationships between groups of parameters) convergence is obtained with 14 parameters, Table 8. Theoretical flapping equation derivatives in fact, compare more favourably with this output-error set of estimates than with any other set in the paper. This result indicates that the 14 derivatives are not entirely independent, and that it is valid to

consider relationships within the model structure. It also serves as a reminder that engineering judgement (in this case, the incorporation of relationships into the model) is a key component in system identification. Results obtained using rank-deficient output-error solutions are fully discussed in Ref. 12.

TABLE 8 -- COMPARISON OF DERIVATIVES IDENTIFIED BY FREQUENCY RESPONSE AND OUTPUT-ERROR METHODS

Derivative	Theoretical Value	Frequency response[1]	Output-error[2,3]
i_{vi}	-9.197	-9.147 (0.0472)	-7.148 (0.38)
.			
$i_{\beta o}$	-36.54	-40.76 (0.5602)	-39.19 (0.50)
i_w	7.311	6.703 (0.0892)	8.360 (0.31)
$i_{\theta o}$	589.0	599.4 (3.0945)	609.9 (0.03)
f_{vi}	-2.294	-4.245 (0.0248)	-3.555 (0.13)
$f_{\beta o}$	-821.9	-836.7 (1.5973)	-804.8 (0.18)
.			
$f_{\beta o}$	-18.75	-24.47 (0.0855)	-22.25 (0.18)
f_w	3.317	4.635 (0.0443)	3.721 (0.57)
$f_{\theta o}$	517.5	682.8 (1.3974)	638.0 (0.11)
Z_{vi}	0.755	0.547 (0.0056)	0.266 (0.06)
$Z_{\beta o}$	-102.3	-96.46 (0.4640)	-112.9 (1.33)
.			
$Z_{\beta o}$	2.868	1.393 (0.0164)	3.766 (0.16)
Z_w	-0.628	-0.474 (0.0315)	-0.627 (0.11)
$Z_{\theta o}$	-79.14	-48.87 (0.3510)	-47.33 (1.09)

[1]parameter standard deviation in parentheses
[2]parameter standard deviation in parentheses
[3]values obtained using rank deficient information matrix (rank 9)

6. DISCUSSION

This Paper has sought to illustrate, by example, some aspects of model identification that can give rise to concerns over whether or not the identified parameters can be used with any confidence for model validation. It is the case however that the key to successful identification in this context lies in the expertise of the user, not only with the identification tools available, but also coupled with a physical understanding of the nature of the model to be validated as well as the experimental data used. Engineering judgement plays perhaps the major part in 'robust' system identification.

The results suggest that models incorporating higher order dynamics do not present any special difficulties in relation to identifiability, if state information is available, and its frequency content covers a range appropriate to the bandwidth of the dynamics of concern. The latter will have an impact on flight experiment design. For example, it could preclude the use of aircraft that cannot be excited by high frequency control inputs because of airworthiness considerations. The actuation system characteristics may be such that they attenuate important higher frequency content in the pilot's input. The aircraft itself may have natural dynamics that are outside the frequency range across which a pilot can apply inputs. This is almost the case for the model structure examined in this Paper, where the coning

mode natural frequency is approximately 3Hz. In the case of the Puma, this means conducting flight tests and identification above 3Hz. With a Lynx or Gazelle however, this figure would rise to 5Hz. It is intended to investigate such topics in the future with the RAE Bedford Lynx helicopter.

Although the Paper's main concern has been the sensitivity of stability and control derivatives to the identification approach used, a model validation result inherent to the analysis of sensitivity, and further to that published previously, is of complementary interest. This concerns the inflow modelling implied by the use of the lift deficiency factor given by equation (10). While the flight results do confirm that the lift deficiency effects ought to be included in the theoretical model, the outstanding discrepancies between theory and flight in the coning and Z-force equation, indicate that the value for C'_l of 0.55 underestimates that implied by the flight results. A value of $C'_l = 0.65$ would resolve the remaining discrepancy between theory and flight. It could be the case that the analytical basis on which the lift deficiency factor (and therefore the inflow model itself) is developed, is inconsistent with the real wake structure. At the relatively low thrust coefficients at which the Puma was flown for the experiments described in this Paper, strong tip vortex and tail rotor interaction effects are present [4]. These effects can be minimised if the rotor is operated at high thrust coefficient [18], and future work should re-examine the validation of a coupled 3 DOF (degree of freedom) model, and the lift deficiency factor given by equation (10), in such a regime.

7. CONCLUSIONS

The general conclusion is that linearised state-space derivative models of helicopter behaviour that incorporate higher order dynamics, can be identified from flight test data with sufficient confidence to allow the results to be used in model validation. While the identified coupled 3 DOF body/coning/inflow model does not exhibit complete robustness to the choice of approach available for this Paper, the use of engineering judgement and an awareness of the theoretical basis of the model to be validated, can minimise to an acceptable extent the specific identifiability concerns highlighted here. The following conclusions can also be made, and relate to the specific items addressed in the Paper.

1. The output-error and transfer function identification and fitting approaches can be used to complement one another. They gave comparable results and either can therefore be used with confidence.

2. The identified model parameters were sensitive to frequency range. This sensitivity tended to diminish above frequencies of 2.5Hz for the inflow and flapping derivatives, and 3Hz for the Z-force terms.

3. The identified model parameters in the dynamic inflow equation are sensitive to variability in the corresponding *a priori* estimates used as initial guesses in the parameter estimation. This can affect the assessment of which value of air mass to use with the theoretical model.

4. Constraining variables to reflect the similarity among derivatives in one of the theoretical models, has little effect on the values of the identified derivatives. However, constraining a variable at a theoretical value can have a substantial impact, that could influence model validation. Full and rank deficient output-error solutions do indicate that the 14 derivatives are not wholly independent, and that some form of relational constraint in the model structure, or constraint derived from the properties of the test data, would be appropriate.

5. With the transfer function matching approach, identified derivatives exhibited substanial sensitivity to test run. This was attributed to the use of identified frequency responses with poor coherence. Use of responses with good coherence, gave identified derivatives that were vastly less sensitive to test run.

8. REFERENCES

1) G D Padfield, Theoretical modelling for helicopter flight dynamics; development and validation. Proceedings of the 16th Congress of the International Council of the Aeronautical Sciences, ICAS 88, Jerusalem, Israel (1988)

2) S S Houston, Identification of factors influencing rotorcraft heave axis damping and control sensitivity in the hover. RAE Technical Report TR88067 (1988)

3) S S Houston, Identification of a coupled body/coning/inflow model of Puma vertical response in the hover. Vertica Vol 13 No 3 (1989)

4) S S Houston, P C Tarttellin, Theoretical and experimental correlation of helicopter aeromechanics in hover. Proceedings of the 45th Annual Forum of the American Helicopter Society, Boston, USA (1989)

5) C G Black, et al, System identification strategies for helicopter rotor models incorporating induced flow. Proceedings of the 14th European Rotorcraft Forum, Milan, Italy (1988)

6) R Bradley, et al, Glauert augmentation of rotor inflow dynamics. Proceedings of the 15th European Rotorcraft Forum, Amsterdam, The Netherlands (1989)

7) G D Padfield, A theoretical model of helicopter flight mechanics for application to piloted simulation. RAE Technical Report TR81048 (1981)

8)D J Murray-Smith, G D Padfield, Robustness issues in rotorcraft system identification. Unpublished RAE material (1989)

9) R T N Chen, W S Hindson, Influence of dynamic inflow on the helicopter vertical response. Vertica Vol 11 Nos 1&2 (1987)

10) W Johnson. Helicopter theory. Princeton University Press (1980)

11) C G Black, D J Murray-Smith, G D Padfield, Experience with frequency-domain methods in helicopter system identification. Proceedings of the 12th European Rotorcraft Forum, Garmisch-Partenkirchen, Fed. Rep. of Germany (1986)

12) C G Black, A frequency-domain output-error identification of a state-space model for heave dynamics (incorporating induced flow) using a limited measurement set. University of Glasgow Dept of Aerospace Engineering Internal Report (in preparation)

13) S S Houston, Lt Cdr R I Horton, The identification of reduced-order models of helicopter behaviour for handling qualities studies. Proceedings of the 13th European Rotorcraft Forum, Arles, France (1987)

14) C G Black, Consideration of trends in stability and control derivatives from helicopter system identification. Proceedings of the 13th European Rotorcraft Forum, Arles, France (1987)

15) R E Maine, K.W. Iliff, Use of Cramer-Rao bounds on flight data with colored residuals. Journal of Guidance, Control and Dynamics, Vol. 4, No. 2 (1981)

16) P J Carpenter, B Fridovitch, Effect of a rapid blade-pitch increase on the thrust and induced-velocity response of a full-scale helicopter rotor. NACA TN 3044 (1953)

17) D M Pitt, D A Peters, Theoretical prediction of dynamic-inflow derivatives. Vertica Vol 5 No 1 (1981)

18) P F Lorber, et al, A comprehensive hover test of the airloads and airflow of an extensively instrumented model helicopter rotor. Proceedings of the 45th Annual Forum of the American Helicopter Society, Boston, USA (1989)